Electronic Structure of Radical Anions and Cations of Polysilanes with Structural Defects

Shu Seki,* Yoichi Yoshida, and Seiichi Tagawa

Institute of Scientific and Industrial Research, Osaka University, 8-1 Mihogaoka, Ibaraki, Osaka 567-0047, Japan

Keisuke Asai

Faculty of Enginnering, University of Tokyo, 7-3-1 Hongo, Bunkyo-ku, Tokyo 113-8654, Japan

Received August 4, 1998; Revised Manuscript Received December 4, 1998

ABSTRACT: The electronic structure of a charged polysilane molecule is studied. The transient absorption spectroscopy was carried out for radical cations and anions of aryl-substituted polysilane molecules with Si-based defects by means of the nanosecond pulse radiolysis technique. Radical cations and anions of polysilanes displayed near-UV and IR absorption maxima at ca. 3.2−3.4 and 0.5−1 eV, respectively. They are ascribed to interband and subband transitions of polaron states and/or charge resonance states (CR) between σ-conjugated segments. The transition energy of the bands was strongly affected by the defects, showing a remarkable blue shift in IR absorption. The energy of the IR absorption band was interpreted as the degree of electron−phonon coupling. The energy rapidly increased from ca. 0.5 eV with an increase in the defect density and saturated at ca. 0.85 eV for radical cations and 0.95 eV for radical anions. It indicated that excess electrons and holes relatively localized at the defect structures, whereas the charges were delocalized in a conjugated segment in linear polysilanes.

Introduction

Silicon and germanium skeleton polymers (for a review, see ref 1) have attracted considerable attention because of the interesting physical properties such as photosensitivity,[2,3] photoconductivity,[4−6] and nonlinear optical properties.[7] Recent experimental results and theoretical calculations on polysilanes have suggested that their conjugated σ-bonding in a silicon skeleton (σ-conjugated system) is responsible for their interesting physical properties.[8−12]

Polysilane derivatives strongly absorb UV light at 300−400 nm, which originates from the $\sigma-\sigma^*$ transition. The UV light exposure effectively causes a photodegradation of Si−Si bonds, giving neutral silyl radicals and a silylene.[13,14] The reaction mechanisms have been thoroughly investigated in terms of their application to photoresist.[15−17] Ionic species of Si-based molecules have also been studied for cyclic and linear polysilanes.[18−20] Cyclic origosilanes form radical anions by reduction with an alkali metal and also form radical cations by oxidation with $AlCl_3$. The ionic species have an unpaired electron delocalized over the silicon skeleton. Charged molecules of polysilanes were produced by a pulse radiolysis technique and displayed chromophores in the near-UV and IR region with very high extinction coefficients.[21,22] The transient spectra suggest that an excess electron or a hole is delocalized over a conjugated segment in a molecule. This indicates that the conjugated molecular orbital (σ-conjugation) is responsible for the absorption spectra of the ionic species.

Organopolysilane solid films show high electric resistance but became p-type semiconductors in the presence of strong electron acceptors.[23] This suggests that the polymer essentially has a semiconducting path for the carriers along a main chain. Thus, an ionized molecule simulates conducting holes or electrons on the silicon chain. Several studies have reported on the energy states of excess electrons on π-conjugated polymers such as polyacetylene.[8−10] They suggested that the polaronic interaction occurs between the electrons and backbone phonons. Recently, the one-electron-theory model has been extended to tetrahedrally bonded polymers as polysilanes and predicted small electron−lattice interaction.[9] The polaron model gives a better interpretation to hole transport in polysilanes; however, the direct observation of the state has not been carried out yet. Thus, transient spectroscopy by the pulse radiolysis technique is useful to elucidate the polaron states on a σ-conjugated system.

A Wurtz coupling reaction of dichlorosilane with alkali metal is often the choice for the polymerization of polysilane derivatives. However, when the polymers are obtained by this method, they contain a small amount of structural defects, such as branching points and oxidated sites. Fujiki reported an empirical linear relationship between the defect density and the relative intensity of broad photoluminescence in the visible region in poly(methylphenylsilane) (PMPS).[24] Hole transport in polysilanes with structural defects was also investigated by microwave absorption and dc time-of-flight techniques.[25,26] The values of charge carrier mobility apparently depended on the density of Si-based defects. This indicates that physical properties of linear polysilanes are dominated by the presence of the structural defects that disturb the σ-conjugated system along a silicon skeleton.

The present paper describes the transient absorption spectra of radical cations and anions of PMPS, PMPS with Si-based structural defects, and poly(phenylsilane) (PPS). The spectra were obtained by the nanosecond pulse radiolysis technique with a wide wavelength range from 300 to 1600 nm. Their optical properties were quantitatively discussed in relation to the amount of Si-based structural defects. The binding energy of excess electrons and holes is estimated on the basis of the polaron model, leading to elucidate the effects of structural defects on the σ-conjugated system in polysilanes.

10.1021/ma981241i CCC: $18.00
Published on Web 01/29/1999

Experimental Section

General. PMPS was synthesized by the conventional sodium condensation (Wultz Coupling) method from the methylphenyldichlorosilane monomer. Defect-containing PMPS was synthesized by same procedure with a monomer mixture of methylphenyldichlorosilane and *p*-toryltrichlorosilane. The ratio of the mixture was changed from 0.15 to 25 wt %. Phenyltrichlorosilane was used as a monomer for the synthesis of PPS with network silicon skeleton. All chlorosilanes were doubly distilled products from Shin-Etsu Chemical Co. Ltd. Polymerization reactions were carried out in an Ar atmosphere, in 100 mL of dry toluene which was refluxed with sodium for 10 h and distilled before use. The monomer was added into the reaction vessel and mixed with sodium dispersion for 12 h. The sodium microdispersion in toluene was purchased from Acros Co. Ltd. PMPS and defect-containing PMPS solutions were precipitated in isopropyl alcohol (IPA) after filtration passing through a 0.45 μm PTFE filter to roughly eliminate NaCl, and precipitates were dried under vacuum. The toluene solutions of these polymers were transferred into a separatory funnel, washed with water to eliminate the remaining NaCl, and precipitated twice with toluene−isopropyl alcohol and tetrahydrofuran (THF)−methanol. PPS was first precipitated by direct addition of IPA into the reaction vessel and then washed with water after filtration. PMPS and defect-containing PMPS showed good solubility for toluene, THF, 2-methyltetrahydrofuran (MTHF), chloroform, and dichloromethane. Because of the less solubility of PPS, the soluble fraction was collected against THF and dichloromethane. The amounts of residual Cl atoms were confirmed to be less than 0.1% in all polysilanes by elemental analysis. The Si-based defect density (D) was confirmed from the ratio of the ^{1}H contents in *p*-tolyl and methyl groups determined by a JEOL EX-270 NMR spectrometer at 270 MHz. ^{29}Si NMR spectra were also recorded using a JEOL EX-600 NMR spectrometer at 120 MHz. The molecular weight distributions in all the polymers were measured with a Shimadzu C-R3A gel permeation chromatography (GPC) system with polystylene calibration standards. Glass transition temperatures were measured with a Perkin-Elmer DSC-7 system. The UV−vis absorption spectra were recorded by a Shimadzu UV-3100 PC system. The photoluminescence spectra were measured with a Perkin-Elmer LS-50B.

Pulse Radiolysis. The pulse radiolysis measurements were performed with an L-band electron linear accelerator at the Radiation Laboratory of the Institute of Scientific and Industrial Research, Osaka University. All the polysilanes were dissolved in THF and CH_2Cl_2 at 0.05 mol/dm^3 concentrated (base mole unit). The THF solutions were evacuated, and the CH_2Cl_2 solutions were bubbled by Ar gas for 5 min before irradiation. The samples were irradiated with a 2 ns single electron pulse at room temperature. A Xe flash lamp was used as a source of analyzing light with a continuous spectrum from 300 to 1600 nm. The analyzing light was monitored with a Ritsu MC-10N monochromator and detected by PIN Si (Hamamatsu S1722) or InGaAs (Hamamatsu G3476) photodiodes. The signals were corrected by a Sony/Tektronics SCD1000 transient digitizer. The typical instrument function was ca. 8 ns.

Low-Temperature Matrix Spectroscopy. The low-temperature matrix experiment was carried out using a ^{60}Co γ-ray source at the ISIR Osaka University. PMPS, PSi (D = 0.0083), and PSi (D = 0.065) were dissolved in MTHF or 2-butyl chloride which was purchased from Dojin Chemical Co. LTD at 10 mM concentrated (base mole unit). We could not perform the experiment for polysilanes with more defects because of the lesser solubility at 77 K against the solvents. The solutions were evacuated and sealed into quartz cells. The irradiation was performed at 77 K and 3.7 kGy/h for 6 h. The samples were exposed to 527 nm laser light after the irradiation to breach the chromophores of trapped solvated electrons in MTHF or radical cations of BuCl. The radical anions and cations of the polysilanes were formed in MTHF and BuCl, respectively, after the breaching.

Table 1. Characteristics of Polysilane Derivatives

entry	feed radio	D^a	$M_w{}^b$	$M_w/M_n{}^c$	$T_g{}^d$ (K)
PMPS	0	0	3.2×10^4	2.3	379
PSi (D = 0.0083)	0.01	0.0083	3.5×10^4	2.6	383
PSi (D = 0.065)	0.07	0.065	2.8×10^4	2.7	385
PSi (D = 0.11)	0.1	0.11	2.6×10^4	3.1	389
PSi (D = 0.23)	0.25	0.23	2.7×10^4	2.9	390
PPS	1	1	4.5×10^4	1.8	

[a] D = Si-based defect density per total Si units. [b,c] M_w and M_n = weight- and number-average molecular weight. [d] T_g = glass transition temperature.

NMR Spectroscopy. PMPS. ^{1}H NMR (270.05 MHz, $CDCl_3$) δ 0.2(br), 7.1(br); ^{29}Si NMR (119.19 MHz, $CDCl_3$) δ −39.2, −39.8, −41.2. PSi (D = 0.0083). ^{1}H NMR (270.05 MHz, $CDCl_3$) δ 0.2(br), 2.3(br), 7.2(br); ^{29}Si NMR (119.19 MHz, $CDCl_3$) δ −39.2, −39.8, 41.2. PSi (D = 0.065). ^{1}H NMR (270.05 MHz, $CDCl_3$) δ 0.2(br), 2.3(br), 7.1(br); ^{29}Si NMR (119.19 MHz, $CDCl_3$) δ −35, −39.2, −39.8, 41.2, −46. PSi (D = 0.11). ^{1}H NMR (270.05 MHz, $CDCl_3$) δ 0.2(br), 2.3(br), 7.2(br); ^{29}Si NMR (119.19 MHz, $CDCl_3$) δ −35, −39.2, −39.8, 41.2, −46. PSi (D = 0.23). ^{1}H NMR (270.05 MHz, $CDCl_3$) δ 0.2(br), 2.3(br), 7.2(br); ^{29}Si NMR (119.19 MHz, $CDCl_3$) δ −35, −39.2, −39.8, 41.2, −46. PPS. ^{1}H NMR (270.05 MHz, $CDCl_3$) δ 7.2(br); ^{29}Si NMR (119.19 MHz, $CDCl_3$) δ −60.

Results and Discussion

Table 1 shows the polymerization results for PMPS, defect-containing PMPS, and PPS. The obtained values of D are proportional to the monomer feed ratio of trichlorosilane and dichlorosilane. A ^{29}Si NMR study on the structural defect-containing polysilanes reported additional broad signals that were ascribed to the Si−Si bond elongation at branching points, suggesting that branching points were actually induced in the polymer main chain.[24] The presence of defects in a main chain is also supported by the changes in glass transition temperatures that increase gradually with increasing D as shown in Table 1. The molecular weights of these polymers used in the present study are also summarized in Table 1. These polysilanes initially show a bimodal molecular weight distribution. Because the number of defects is predicted to depend on the molecular weight of PMPS,[24] the high molecular weight fraction was eliminated. This gives the small dispersion and the similar value of their molecular weights.

Figure 1 shows the absorption spectra of the polysilanes in THF. The absorption maxima shift from 337 to 332 nm with increasing D. PPS has no peak at the region with a tail observed over 400 nm. An extinction coefficient at the absorption maximum was decreased from 9.2×10^3 to 4.8×10^3 with increase in D from 0 to 0.23. A full width of half-maximum (fwhm) of the band also changes from 0.22 eV for PMPS to 0.31 eV for PSi (D = 0.23), respectively. The UV absorption of PMPS was already ascribed to the transition exciton states in a Si conjugated segment. The present results indicate that defect structure increases the energetic dispersion of the exciton state.

Photoluminescence spectra of the polysilanes are illustrated in Figure 2. Defect-containing polysilanes show two emission bands: S emission observed at around 370 nm with a fwhm of ca. 0.1 eV and B emission in the visible region with a large fwhm of ca. 0.7−1 eV. The B emission shows a remarkable red shift and becomes broader with increase in D. The S emission was ascribed to a relaxation process of exciton states. As reported previously, the excitation spectrum of B emission is not identical to the absorption spectrum of the

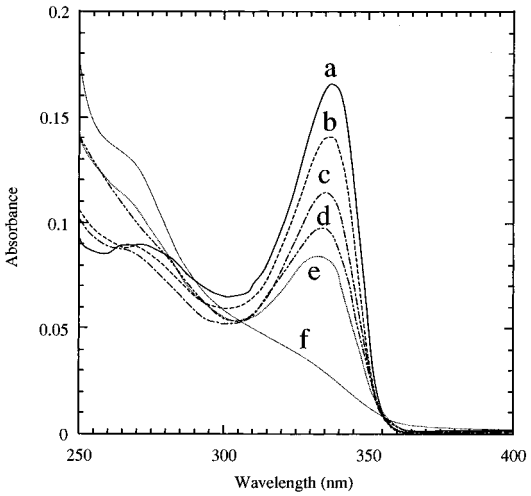

Figure 1. Absorption spectra of polysilanes in a THF solution at 2.0×10^{-5} mol/dm^3 concentrated (base mole unit): (a) PMPS, (b) PSi ($D = 0.0083$), (c) PSi ($D = 0.065$), (d) PSi ($D = 0.11$), (e) PSi ($D = 0.23$), and (f) PPS.

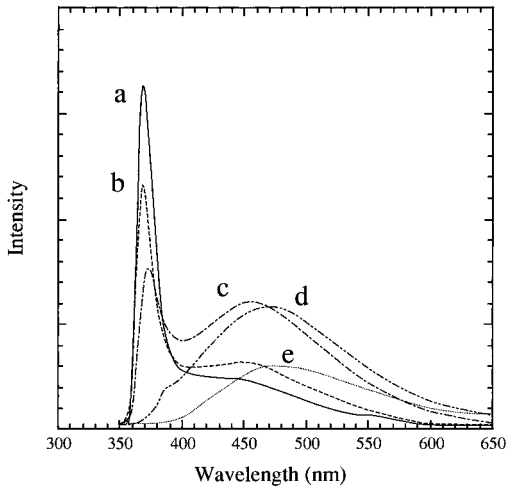

Figure 2. Fluorescence spectra of polysilanes in a THF solution: (a) PSi ($D = 0.0083$), (b) PSi ($D = 0.065$), (c) PSi ($D = 0.11$), (d) PSi ($D = 0.23$), and (e) PPS.

polymer but exhibits a broad band around 4 eV with a tail ranging to ca. 3 eV. This indicates that a different energy state on Si main chain is responsible for the B emission, such as the localized exciton states at defect structures. It is also supported by the presence of tail structures in absorption spectra of defect-containing polysilanes.

Transient spectroscopy of radical anions and cations of the polysilanes was performed by means of the electron beam pulse radiolysis. In each THF or dichloromethane solution, incident electrons cause the reactions as illustrated in Figure 3. The anionic or cationic species of polysilanes are then formed within an electron pulse width (fwhm = 8 ns). The observed transient spectra in THF and CH_2Cl_2 are shown in Figures 4 and 5 for PMPS and PSi ($D = 0.025$), respectively. Two absorption bands are observed in near-UV (UV band) and IR (IR band) regions for both radical anions and cations of the polymers. Both UV and IR bands indicate a similar time dependence for all cases as shown in the superimposed figures. The maximum of the IR band was confirmed by the low-temperature matrix experiment as displayed in Figure 6 for radical anions of PMPS and PSi ($D = 0.0083$). The transition energies of the UV band (E_{UV})

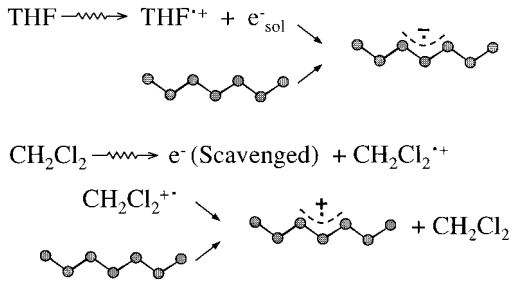

Figure 3. Scheme of the reaction and the resulting polymer radical anions and cations. The polymer molecule is simply represented by the skeleton of catenating Si atoms.

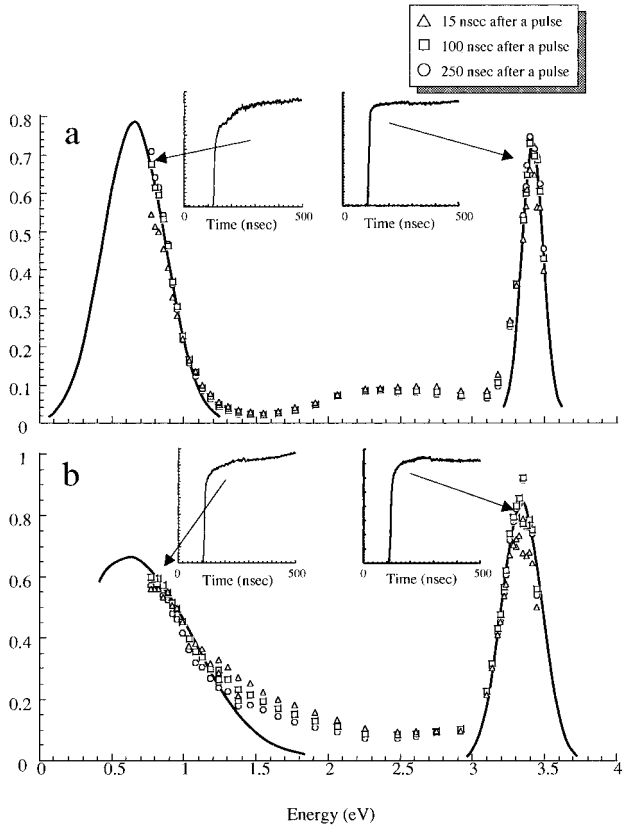

Figure 4. Transient absorption spectra of radical anions (a) and radical cations (b) of PMPS at 15, 100, and 250 ns after a pulse. Superimposed figures indicate the kinetic traces of transient absorption.

and IR band (E_{IR}) were 3.36 and 0.59 eV, respectively, for PMPS radical anions. The sum of the two absorption energies becomes ca. 3.95 eV, showing good agreement with calculated band gap energy (E_g) in PMPS. For cations of PMPS, E_{UV} and E_{IR} were estimated to be 3.41 and 0.55 eV, also indicating the same total transition energy as E_g. This suggests the presence of an interband level occupied by an excess electron or a hole.

The width of UV and IR bands decreased with the observation time in Figures 4 and 5. The shrinking suggests the decrease in the energetic dispersion of interband levels. A polysilane molecule already revealed having a backbone consisting of conjugated helical segments joined to each other by a disordered part. An excess electron or a hole on a polymer migrates into the most stable conjugated segment within the observation time range; thus, the intersegment charge transfer may be responsible for the decrease in the dispersion.

Figure 7 shows a series of transient absorption spectra observed for radical anions of the polymers. The

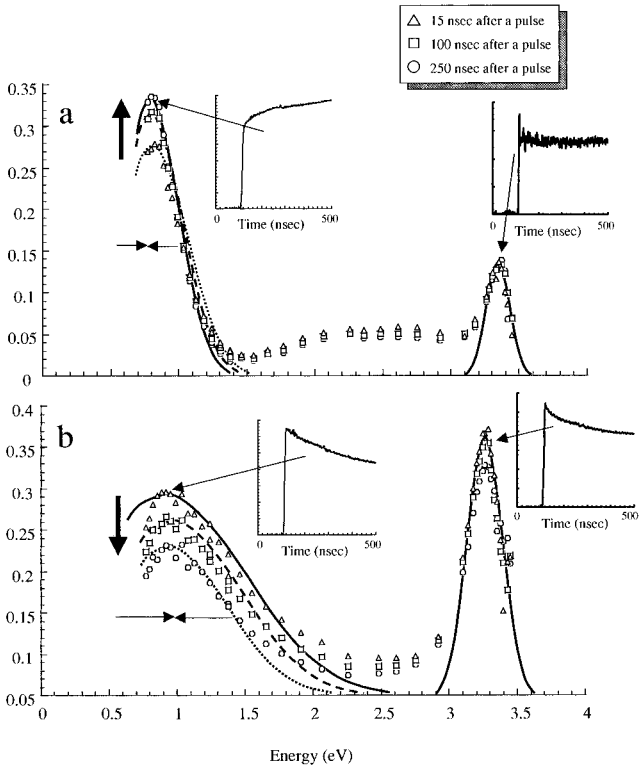

Figure 5. Transient absorption spectra of radical anions (a) and radical cations (b) of PSi (D = 0.23) at 15, 100, and 250 ns after a pulse. Superimposed figures indicate the kinetic traces of transient absorption.

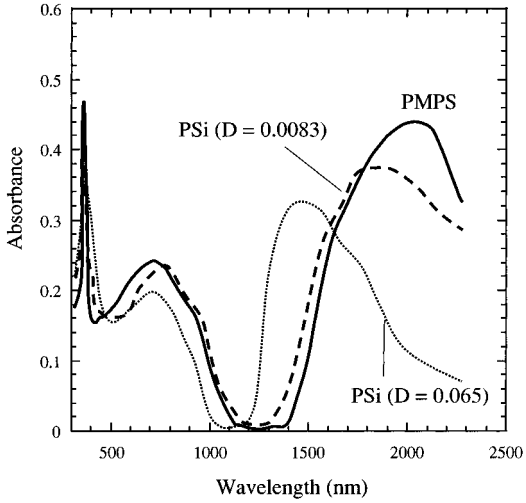

Figure 6. Absorption spectra of polysilanes in MTHF solutions at 77 K. The solutions were irradiated by ^{60}Co γ-rays at 15.7 kGy, and solvated electrons were breached by the exposure to a 527 nm laser light for 1 min. Solid, dashed, and dotted lines indicate the spectra of PMPS, PSi (D = 0.0083), and PSi (D = 0.065), respectively.

spectra of radical cations are also shown in Figure 8. The UV band slightly shifts to longer wavelength region with increasing D over 0.065. In contrast, the IR band presents a remarkable blue shift with increase in D. The absorption energies of UV and IR bands are summarized in Table 2. The value of E_{IR} estimated for PSi (D = 0.065) by the matrix experiment corresponds to that observed by the pulse radiolysis as shown in Figures 6 and 7. The sum of E_{UV} and E_{IR} is almost same for both cations and anions of a polymer. The total transition energy presents E_g that increases from 3.9 to 4.2 eV

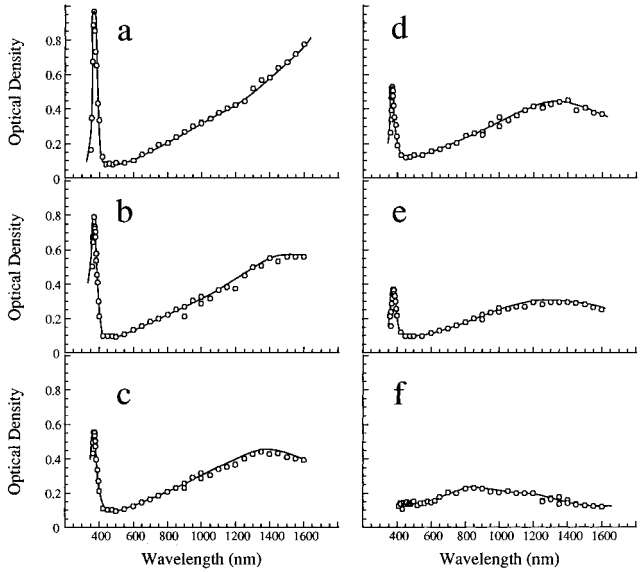

Figure 7. Transient absorption spectra of radical anions of the polymers at 15 ns after a pulse: (a) PMPS, (b) PSi (D = 0.0083), (c) PSi (D = 0.065), (d) PSi (D = 0.11), (e) PSi (D = 0.23), and (f) PPS.

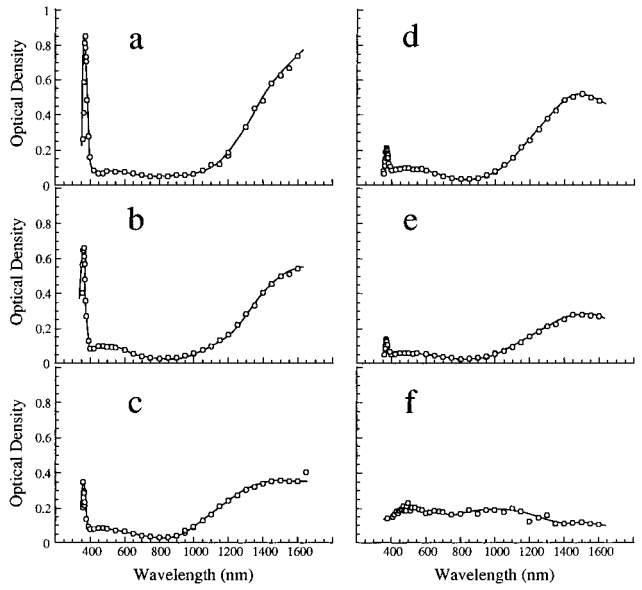

Figure 8. Transient absorption spectra of radical cations of the polymers at 15 ns after a pulse: (a) PMPS, (b) PSi (D = 0.0083), (c) PSi (D = 0.065), (d) PSi (D = 0.11), (e) PSi (D = 0.23), and (f) PPS.

with increasing D from 0.0 to 0.23. The IR band reflects the subband transition between the valence band and interband levels in the radical anions and also reflects the transition between interband levels and conduction band in the radical cations. The present pulse radiolysis technique predominately produces singly charged molecules; thus, the interband level may be promoted by polaron interaction between a charge and phonons in a silicon skeleton and/or charge resonance (CR) interaction between two adjoining σ-conjugated segments. Because of the same total transition energy as E_g in PMPS and little difference in the total energy of radical cations and anions, the polaron interaction is responsible for the formation of the interband levels. Thus, E_{IR} denotes the binding energy ($\delta\epsilon$) of a polaron state on a Si segment. The value of $\delta\epsilon$ gradually increases with increasing D and saturates at 0.95 and 0.86 eV for the

Table 2. Transient Absorption Bands of Polysilane Derivatives

D	anion IR λ_{max} ($\times 10^3$ nm)	λ_{max} energy (eV)	cation IR λ_{max} ($\times 10^3$ nm)	λ_{max} energy (eV)
0	2.10[a]	0.59	2.25[a]	0.55
0.0083	1.90[a]	0.65	2.05[a]	0.60
0.065	1.47	0.84	1.55	0.80
0.11	1.40	0.89	1.50	0.82
0.23	1.30	0.95	1.45	0.86
D	anion UV λ_{max} (nm)	λ_{max} energy (eV)	cation UV λ_{max} (nm)	λ_{max} energy (eV)
0	369	3.36	364	3.41
0.0083	370	3.35	364	3.41
0.065	369	3.36	366	3.39
0.11	373	3.31	368	3.37
0.23	379	3.25	372	3.33

[a] The values of λ_{max} were determined by the low-temperature matrix experiment.

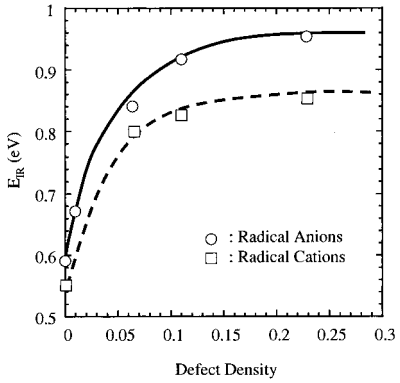

Figure 9. Dependence of E_{IR} on *D*. Circles indicate E_{IR} of radical anions, and squares indicate E_{IR} of radical cations.

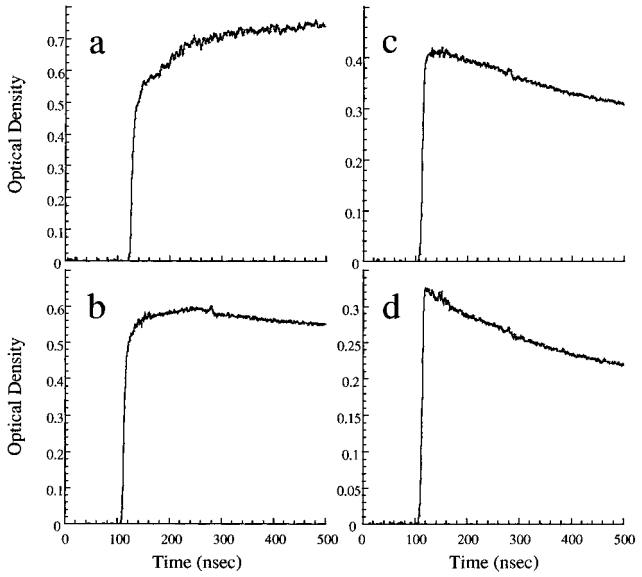

Figure 10. Kinetic traces of transient absorption of the radical anions in the IR region: (a) PMPS monitored at 1600 nm, (b) PSi ($D = 0.065$) monitored at 1450 nm, (c) PSi ($D = 0.11$) monitored at 1350 nm, and (d) PSi ($D = 0.23$) monitored at 1250 nm.

anions and the cations as shown in Figure 9. The kinetic traces of the IR band are summarized in Figures 10 and 11 for radical cations and anions, respectively. The IR band attributed to the radical anions decays faster when the polymer contains the large number of defects, while showing the same kinetic traces for radical cations. The molecular weight of the polymers was monitored before

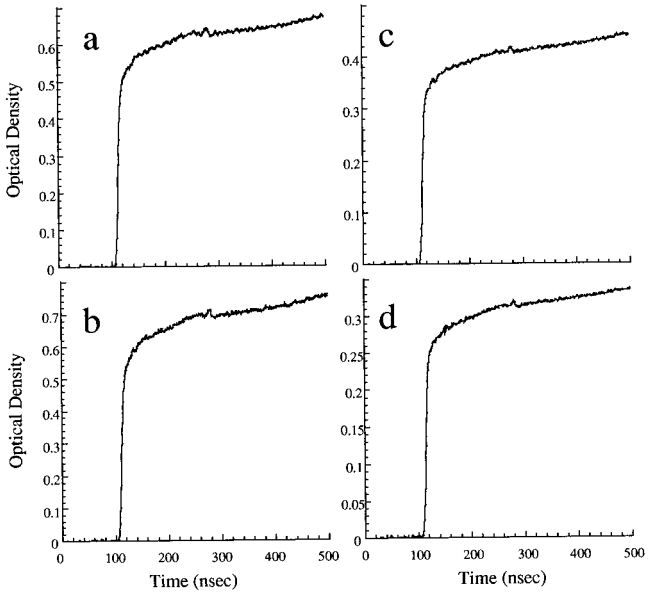

Figure 11. Kinetic traces of transient absorption of the radical cations in the IR region: (a) PMPS monitored at 1600 nm, (b) PSi ($D = 0.065$) monitored at 1550 nm, (c) PSi ($D = 0.11$) monitored at 1500 nm, and (d) PSi ($D = 0.23$) monitored at 1400 nm.

and after the irradiation to the THF solutions. The *G* values (number of reactions per absorbed 100 eV) of main chain scission is estimated as 0.087 and 0.23 for PMPS and PSi ($D = 0.23$), respectively. This indicates that the radical anion may be a precursor of a chain scission reaction, and an excess electron is localized at the defect on a silicon skeleton, leading to side and/or main chain dissociation reactions.

Several groups have studied the electronic states of conjugated polymer chains with unpaired electrons, suggesting polaron, bipolaron, and charge neutral polaron states.[8−10] It was predicted that the lattice relaxation played a crucial role in determining the state of an electron or a hole on a conjugated polymer chain, such as polyacetylenes.[8,10] Based on the Sandrofy C model (for a review, see ref 27), the following formula is obtained as the relation between the polaron width and the binding energy:

$$\delta\epsilon \approx \left(\frac{\Delta V}{2\alpha}\right)\left(\frac{a}{\xi_p}\right)^2 \tag{1}$$

where $\delta\epsilon$ denotes the binding energy of a polaron, *a* denotes a lattice unit of a trans-chain segment, and ξ_p is the polaron width. *V* is the matrix element describing the interaction between two atomic orbitals consisting a covalent bond, and Δ also denotes the matrix element between two atomic orbitals of a Si atom. α is represented by

$$\alpha \equiv [V(r) - \Delta] \tag{2}$$

$$r = \frac{a}{\sin\theta} \tag{3}$$

where 2θ is the tetrahedral bond angle. Thus, Δ is a parameter which specifies the degree of delocalization of σ electrons on a σ-conjugated segment while *V* described the localization of a pair of electrons in a local bond.

The relative polaron width on the polymers can be estimated based on eq 1. With the previously reported

Table 3. Relative Extinction Coefficients of the UV Band

D	rel ϵ at λ_{max} of radical anions	rel ϵ at λ_{max} of radical cations
0	1.0	1.0
0.0083	0.80	0.76
0.065	0.58	0.42
0.11	0.54	0.26
0.23	0.39	0.16

values of Δ and V in poly(dimethylsilane), the value of ($\Delta V/2\alpha$) can be estimated as ca. 1 eV.[28,29] The observed binding energy of positive and negative polarons is also ca. 1 eV in the polymer containing high defect density such as PSi ($D = 0.23$), giving $\xi_p/a \sim 1$. It suggests the highly polarized polaron state localized on a single Si unit. The polaron relatively delocalizes on a Si conjugated segment in the polysilanes with fewer defects because of the smaller values of $\delta\epsilon$.

The aryl-substituted polysilanes with Si-based defect structures were already reported to show a broad emission band around 2.9 eV.[24] The intensity of the new emission band had a good empirical relation to the amount of silicon branching in the backbone. The density of silicon branching in a PMPS was estimated at <1% considering the relative emission intensity. We also reported the amount of silicon branching in a PMPS obtained by the Wurtz coupling reaction. It was less than 3.5%, which was determined by EPR spectroscopy for silyl radicals that migrated into branching points.[30,31] The potential density of defects in a PMPS was also estimated by the empirical relationship between the hole drift mobility and the defect density, leading to be the value of 0.14%. In the present study, the relative extinction coefficient of the UV band, ϵ_{rel}, is remarkably affected by the presence of structural defects as shown in Figures 7 and 8 and as summarized in Table 3. Figure 12 displays a semilogarithmic plotting of E_{IR} and ϵ_{rel} vs D. By the fitting of the plotting, the following empirical formulas were obtained:

$$\epsilon_{rel} = 0.25 - 0.27 \log D \quad (4)$$

$$\epsilon_{rel} = -0.11 - 0.42 \log D \quad (5)$$

where eq 4 is obtained as the relation in radical anions, and eq 5 also represents the relation in radical cations. $\epsilon_{rel} = 1$ gives the potential density of defects in the PMPS used in the present study, giving $D = 1.7 \times 10^{-3}$ from eq 4 and 2.2×10^{-3} from eq 5. The plotting of E_{IR} vs D also gives the following formula:

$$E_{IR} = 1.1 + 0.21 \log D \quad (6)$$

$$E_{IR} = 1.0 + 0.19 \log D \quad (7)$$

They are respectively obtained as the relation of radical anions and cations. The values of D in the PMPS are evaluated by $E_{IR} = 0.59$ in eq 6 and $E_{IR} = 0.55$ in eq 7, suggesting $D = 4.1 \times 10^{-3}$ and $D = 4.2 \times 10^{-3}$. Thus, when the Wurtz coupling reaction is used to synthesize the polysilanes, it is still difficult to prevent the polymer from induced defect structure. However, the molecular weight of the polymer ($M_w = 3.2 \times 10^4$, $M_n = 1.8 \times 10^4$) suggests the degree of polymerization to be a few hundred. Therefore, a few defect structures are maximally present in a PMPS molecule.

Conclusion

The electronic states of excess electrons or holes were investigated by the nanosecond pulse radiolysis technique. Transient absorption spectroscopy was carried out for radical cations and anions of polysilanes with Si-based defect structures. The radical cations and anions of polysilanes displayed near-UV and IR absorption maxima at ca. 3.2−3.4 and 0.5−1 eV, respectively. They are ascribed to the interband and the subband transition of polaron states. The values of E_{UV} and E_{IR} were strongly affected by the defect density, showing a remarkable blue shift in IR absorption. The E_{IR} was interpreted as the degree of electron−phonon coupling which rapidly increased with increasing defect density and saturated at ca. 0.85 eV for radical cations and 0.95 eV for radical anions. This indicates that excess electrons and holes are localized at the defect structures in specimens with more defects, while the charge was relatively delocalized in a conjugated segment in the polysilanes with fewer defects. We obtain the empirical relation between E_{IR} and D, also between ϵ_{rel} and D, giving the potential density of Si-based defect structures in PMPS as $(1-5) \times 10^{-3}$.

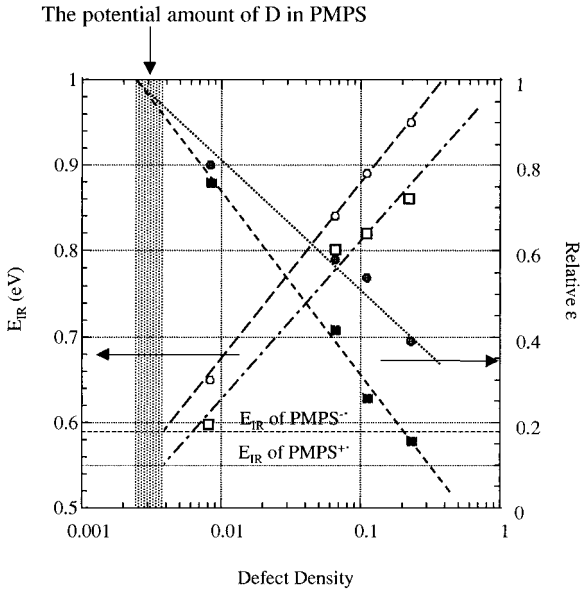

Figure 12. Semilogarithmic plotting of E_{IR} and ϵ_{rel} vs D. The thresholds denote the measured E_{IR} of radical anions and cations of PMPS, which was obtained from the conventional Wurtz coupling reactions without using trichlorosilanes.

Acknowledgment. The authors acknowledge Dr. T. Kozawa at ISIR Osaka University for the experimental support. We also acknowledge Dr. A. D. Trifunac, Dr. K. R. Cromack, Dr. D. Wurst, and Dr. C. D. Jonah at Argonnne National Laboratory and Dr. H. Kudoh at Japan Atomic Energy Research Institute for their useful advise. This work was supported by a Grant-in-aid for scientific research No. 09239230 from the Ministry of Education, Science and Culture.

References and Notes

(1) Miller, R. D.; Michl, J. *Chem. Rev.* **1989**, *89*, 1359.
(2) Zeigler, J. M.; Harrah, L. A.; Johnson, A. W. *Proc. SPIE* **1985**, *536*, 166.
(3) Hofer, D. C.; Miller, R. D.; Willson, C. G. *Proc. SPIE* **1984**, *246*, 16.
(4) Kepler, R. G.; Zeigler, J. M.; Harrah, L. A.; Kurtz, S. R. *Phys. Rev.* **1987**, *B35*, 2818.
(5) Fujino, M. *Chem. Phys. Lett.* **1987**, *136*, 451.
(6) Stolka, M.; Yuh, H. J.; McGrane, K.; Pai, D. M. *J. Polym. Sci., Polym. Chem. Ed.* **1987**, *25*, 823.
(7) Kajar, F.; Messier, J.; Rosilo, C. *J. Appl. Phys.* **1986**, *60*, 3040.

(8) Su, W. P.; Schrieffer, J. R.; Heeger, A. J. *Phys. Rev. Lett.* **1979**, *58*, 937.
(9) Rice, M. J.; Phillpot, S. R. *Phys. Rev. Lett.* **1987**, *58*, 937.
(10) Rice, M. J. *Phys. Lett.* **1979**, *A71*, 152.
(11) Phillpot, S. R. *Phys. Lett.* **1987**, *31*, 43.
(12) Takeda, K.; Fujino, M.; Seki, K.; Inokuchi, H. *Phys. Rev.* **1987**, *B36*, 8129.
(13) Trefonas, P.; West, R.; Miller, R. D.; Hofer, D. *J. Polym. Sci., Polym. Lett. Ed.* **1983**, *21*, 823.
(14) Trefonas, P.; West, R.; Miller, R. D. *J. Am. Chem. Soc.* **1985**, *107*, 2737.
(15) Zeigler, J. M.; Harrah, L. A.; Johnson, A. W. *Proc. SPIE* **1985**, *539*, 166.
(16) Hofer, D. C.; Miller, R. D.; Willson, C. G. *Proc. SPIE* **1984**, *469*, 16.
(17) Taylor, G. N.; Wolf, W. W.; Moran, J. M. *J. Vac. Sci. Technol.* **1981**, *19*, 872.
(18) West, R.; Carberry, E. *Science* **1975**, *189*, 179.
(19) Carberry, E.; West, R.; Glass, G. E. *J. Am. Chem. Soc.* **1969**, *91*, 5446.
(20) Kira, M.; Bock, H.; Hengge, R. *J. Organomet. Chem.* **1979**, *164*, 277.
(21) Ban, H.; Sukegawa, K.; Tagawa, S. *Macromolecules* **1987**, *20*, 1775.
(22) Ban, H.; Sukegawa, K.; Tagawa, S. *Macromolecules* **1988**, *21*, 45.
(23) West, R.; David, L. D.; Djurovich, P. I.; Stearly, K. L.; Srinivasan, K. S. V.; Yu, H. *J. Am. Chem. Soc.* **1981**, *102*, 7352.
(24) Fujiki, M. *Chem. Phys. Lett.* **1992**, *198*, 177.
(25) van Walree, C. A.; Cleiji, T. J.; Jenneskens, L. W.; Vlietstra, E. J.; van der Laan, G. P.; de Haas, M. P.; Lutz, E. G. *Macromolecules* **1996**, *29*, 7362.
(26) Seki, S.; Yoshida, Y.; Tagawa, S.; Asai, K.; Ishigure, K.; Furukawa, K.; Fujiki, M.; Matsumoto, N. *Philos. Mag. B*, submitted for publication.
(27) Pitt, C. G. In *Homoatomic Rings, Chains, and Macromolecules of Main Group Elements*; Rheingold, A. L., Ed.; Elsevier: Amsterdam, 1977.
(28) Kumada, M.; Tamao, K. *Adv. Organomet. Chem.* **1968**, *6*, 80.
(29) Pollard, W. B.; Lucovsky, G. *Phys. Rev.* **1982**, *B26*, 3172.
(30) Seki, S.; Cromack, K. R.; Trifunac, A. D.; Yoshida, Y.; Tagawa, S.; Asai, K.; Ishigure, K. *J. Phys. Chem. B* **1998**, *102*, 8367.
(31) Seki, S.; Cromack, K. R.; Trifunac, A. D.; Tagawa, S.; Ishigure, K.; Yoshida, Y. *Radiat. Phys. Chem.* **1993**, *47*, 217.

MA981241I